New mechanism of structuring associated with the quasi-merohedral twinning by an example of $Ca_{1-x}La_xF_{2+x}$ ordered solid solutions

© S. Maksimov[+], K. Maksimov*¶, N. Sukhov‡, M. Lovygin[+]

[+] National Research University MIET (Laboratory of EMI),
124498 Moscow, Russia
* Institute VIMI FSUE,
125993 Moscow, Russia
‡ Moscow State University (Faculty of Physics),
119991 Moscow, Russia

(Получена 24 марта 2015 г. Принята к печати 30 марта 2015 г.)

Merohedry is considered an inseparable property of atomic structures, and uses for the refinement of structural data in a process of correct determination of structure of compounds. Transformation of faulty structures stimulated by decreasing of systemic cumulative energy leads to generation of merohedral twinning type. Ordering is accompanied by origin of antiphase domains. If ordering belongs to the CuAu type, it is accompanied by tetragonal distortions along different ⟨100⟩ directions. If a crystal consists of mosaic of nanodimensional antiphase domains, the conjugation of antiphase domains with different tetragonality leads to monoclinic distortions, at that, conjugated domains are distorted mirrorly. Similar system undergoes further transformation by means of quasi-merohedral twinning. As a result of quasi-merohedry, straight-lines of lattices with different monoclinic distortions are transformed into coherent lattice broken-lines providing minimization of the cumulative energy. Structuring is controlled by regularities of the self-organization. However stochasticity of ordering predetermines the origin areas where few domains with different tetragonality contact which leads to the origin of faulty fields braking regular passage of structuring. Resulting crystal has been found structurally non-uniform, furthermore structural non-uniformity permits identifying elements and stages of a process. However there is no precondition preventing arising the origin of homogenous states. Effect has been revealed in $Ca_{1-x}La_xF_{2+x}$ solid solution, but it can be expected that distortions of regular alternation of ions similar to antiphase domains can be obtained in non-equilibrium conditions in compounds and similar effect of the quasi-merohedry can falsify results of structural analysis.

1. Introduction

The only contribution of deliberate technologies was obtaining of compositions with a specified content. All other steps of structuring: ordering of the CuAu type, origin of structure of antiphase domains with different tetragonality directions, relaxation misfit stresses by means of conjugation of domains with different tetragonality directions leading to pairs of mirrorly symmetric monoclinic structures, relaxation of stresses associated with 2 types of monoclinity by means of merohedral [1] twinning are determined by minimization of the cumulative energy [2].

Ordering is a stochastic process that is accompanied by the emerging of antiphase domains (APDs).[1] CuAu ordering in FCC structures or structures coming from FCC also favours the origin of domains differed by directions of alternation of components along different ⟨100⟩ directions (DACDs) [3]. Nanostructuring depends on the relaxation of the surface energy therefore it can also be associated with relaxation of energy of antiphase domain boundaries (APBs). Ordering of Ca^{+2} and La^{+3} ions in cation sublattice and antiphase domain structure was revealed in studies of $Ca_{1-x}La_xF_{2+x}$ crystals [4,5], and these crystals are opportune objects for investigations of the APB role in structuring.[2]

If two volumes are separated by two boundaries of different types, superposition of resulting amplitudes of scattering (of X-rays, electrons, neutrons) inherent to these volumes must reflect total displacement at these boundaries. There exist two types of boundaries that provoke displacements: twin boundaries (TBs) and APBs. TB changes relative orientation of one part of a crystal with respect to another, i.e., affects the crystal as a whole [6]. Transition through APD changes regularities of component alternations and leads only to step-wise changes of phases of superstructure reflections; structure reflections are not responsive to antiphase boundaries. Therefore it follows to expect that the coexistence APD and twins must only have an influence, as a first approximation, on intensities of superstructure reflections [7].

$Ca_{0.65}La_{0.35}F_{2.35}$ and $Ca_{0.5}La_{0.5}F_{2.5}$ solid solutions with lattices on the base of the cubic CaF_2 lattice are formed as a result of a high-temperature annealing [4,5]. As the result of the annealing, they gain APD structure associated with ordered Cu^{+2} and La^{+3} distribution on positions of the cation sublattice. APD structuring in $Ca_{1-x}La_xF_{2+x}$ is

¶ E-mail: maksimov_sk@akado.ru, kuros@rambler.ru

[1] APD, DACD, APDB, TwB, and so on are notations corresponding to a singular object, APDs, DACDs, APDBs, TwBs, and so on are notations corresponding to their multitudes.

[2] All specimens were obtained in Institute of Crystallography RAS and were kindly given by B.P. Sobolev.

accompanied by intensive twinning with a nanodimensional scale [4]. Ordering in $Ca_{1-x}La_xF_{2+x}$ falls into the CuAu type and is accompanied by considerable distortions of unit cells due to large distinctions of La^{+3} and Ca^{+2} ion radii [8], that must simplify the revelation of effects associated with interaction between APBs and TBs with specific location planes. We have tried to study summing effects of coexistence of TBs and ATBs by means of electron diffraction patterns of $Ca_{1-x}La_xF_{2+x}$, but we faced an effect, analogues to which are evidently not known for scientists. Its peculiarities and unusualness are especially evident when the results belonging to $Ca_{0.65}La_{0.35}F_{2.35}$ (where it is impossible) [4] and $Ca_{0.5}La_{0.5}F_{2.5}$ (where it is observed) [5] are compared. Superstructure reflections are not observed for both phases if thickness (d) exceeds 20 nm, as a result of APD structure averaging over a scattering volume, but they are observed if $d < 15$ nm. Motive force of structuring of both the phases is the ordering of CuAu type therefore they are crystalline and chemically identical during early annealing stages. However regularities of their structuring diverge with increase of annealing timing [4,5,8,9].

Transition of the initial CuAu structure in $Ca_{0.65}La_{0.35}F_{2.35}$ and $Ca_{0.5}La_{0.5}F_{2.5}$ with time is realized by different ways that demand involvement of different effective forces. $Ca_{0.65}La_{0.35}F_{2.35}$ composition is remote from the equilibrium $Ca_{0.5}La_{0.5}F_{2.5}$ therefore in $Ca_{0.65}La_{0.35}F_{2.35}$ precipitation of the equilibrium $Ca_{0.65}La_{0.35}F_{2.35}$ phase is possible. Misfit stresses at boundaries precipitate/matrix determine in many respects processes of subsequent. $Ca_{0.5}La_{0.5}F_{2.5}$ composition corresponds to the maximum solubility of LaF_3 in CaF_2. Therefore compositional segregation and precipitation in the $Ca_{0.5}La_{0.5}F_{2.5}$ are impossible, and APD structure remains intact. Therefore other effective forces act in $Ca_{0.5}La_{0.5}F_{2.5}$ [7]. Maximal values come up, firstly, with stresses associated with the conjugation of DACDs with different tetragonality directions, secondly, with the energy density accumulated in APBs. If we take into account together the density of cut bonds and also electrostatic energy of La^{+3} and Ca^{+2}, then density energy accumulated by APD with sizes that achieve 3 nm can be estimated to $120-180\,J\cdot cm^{-3}$ [3,9]. Such energy is, possibly, not enough for the relaxation by means of generation of defect structure solely, but APD can simplify its origin and become a substrate to its origin.

Electron diffraction patterns obtained with a use of the selective diaphragm measuring $0.5\,\mu$m (SED technique — selective electron diffraction) permit the averaging of diffraction data for large volumes. SED has been chosen as the basic investigation method for revealing peculiarities of electron diffraction patterns in this paper. Electron microscopy (TEM and HRTEM) had been used for obtaining the additional information. Fourier transforms (FFT) and inverse FFT (IFFT) were used for the explanation of the essence and restructuring going with annealing.

Specimens were obtained by spalling along twinning planes.

2. $Ca_{0.65}La_{0.35}F_{2.35}$ structuring

Typical $Ca_{0.65}La_{0.35}F_{2.35}$ structuring is reflected by Fig. 1. Visible peculiarities of $Ca_{0.65}La_{0.35}F_{2.35}$ structuring in SED are superstructure reflections and satellites. Intensive twinning is also observed in TEMs. Typical twins have sizes measuring $\sim (3.0-10)$ nm. Cause and mechanism of twin generation is illustrated by Fig. 1, *c*, where precipitate initiating stresses in the matrix and twins arising as the result are seen. Precipitate has a habit going back to cubooctahedron. Twins with $\{111\}$ location planes are born along edges of intersection of $\{100\}$ and $\{111\}$ facets. Twins are oriented along bisector of angle produced by $\{100\}$ and $\{111\}$ facets, serving as a reason of their initiation. Fig. 1, *b* is covered by twin images as a whole. Silhouettes of precipitates shown by arrows are seen over all the Fig. 1, *b*. Precipitate sizes are nanodimensional and, as it will be seen further, are similar to sizes of APD in $Ca_{0.5}La_{0.5}F_{2.5}$. Similarity of sizes allows us to claim that precipitates can evolve from APD. However APD in $Ca_{0.5}La_{0.5}F_{2.5}$ have shapes going back to a hexagonal prism or cubic-rhombic-dodecahedron. Changes of habit and stresses associated with precipitates provoking twinning indicate that APD structure is differing from matrix structure. Any diffraction manifestations of precipitation in SED are absent. Only distinctions of $La_{0.5}Ca_{0.5}F_{2.5}$ SEDs from CaF_2 diffraction patterns are SStRs, which are observed only in very thin areas [4,5]. Therefore precipitate structure can be close to matrix structure. Misfit stress field has the symmetry corresponding to the matrix symmetry [5.6]. Reflection intensity in SED decreases monotonically with distance from the zero series.

Precipitation develops from APD by means of the interdiffusion, which brings La^{+3} content of some APD to equilibrium 50% and increases Ca^{+2} content in the matrix. Composition changes lead to variations of lattice constants, those are accompanied by the initiation of misfit stresses, and surface tension energy is minimized by the change of the habit with the subsequent relaxation of the misfit stresses by means of twinning. Twins have a thickness equal to 2 nm, and scattered waves leave rapidly a twin body, therefore only and only twin reflections with small diffraction vectors **g** are observed in SED. All mechanisms of twinning in a solid crystal are associated expressly or by implication with stacking faults. The highest twin density and lack of dislocations are evidence of extremely small the stacking fault energy in $Ca_{1-x}La_xF_{2+x}$ [3,6]. Precipitation and twinning lead to coarsening of the initial APD structure.

3. $Ca_{0.5}La_{0.5}F_{2.5}$ structuring

Structuring of 2nd type is observed for $Ca_{0.5}La_{0.5}F_{2.5}$.

The volume selected in this studies contains (110) and (101) twins with the same [100] direction of tetragonal distortions and (011) twins having the [010] tetragonal directions. As reference projections, there were selected: the

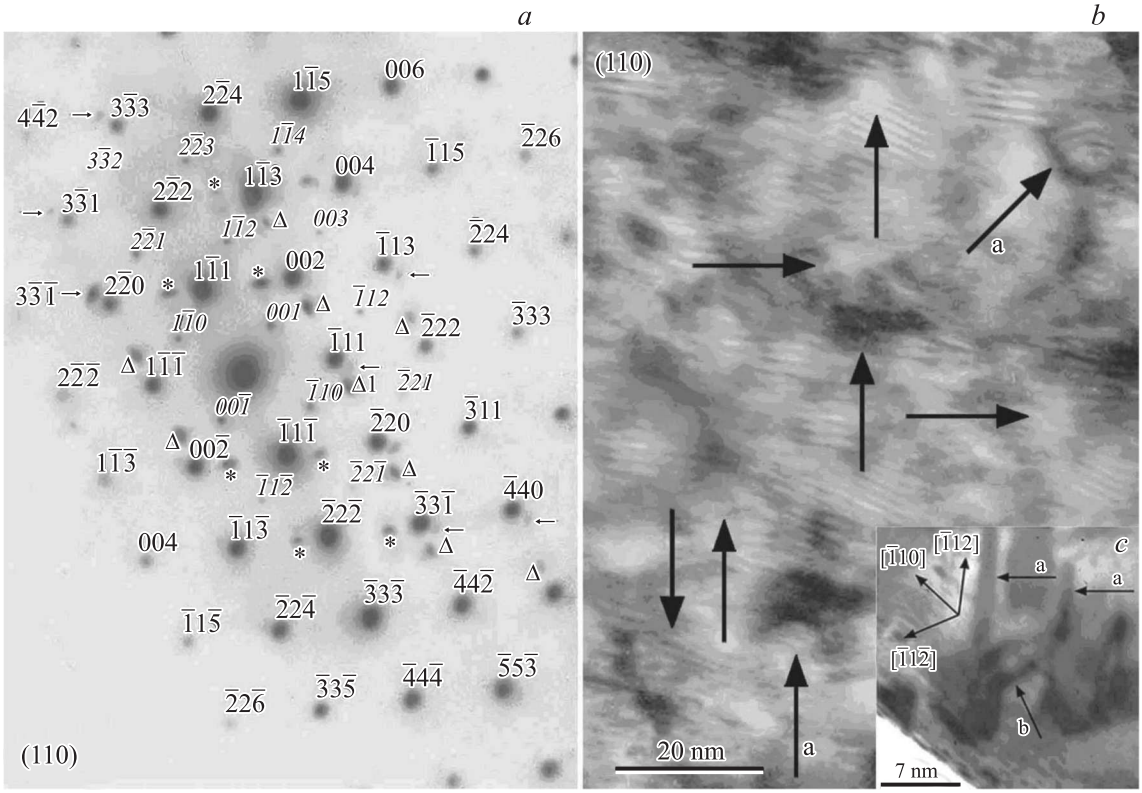

Figure 1. Peculiarities of $Ca_{0.65}La_{0.35}F_{2.35}$ structuring. *a* — SED corresponding to [110] projection of area with thickness equal approximately 20 nm; indices of structure reflections (StRs) are marked by Roman type, those of superstructure reflections (SStRs) are done by italics; * are reflections of (101) twins, Δ are reflections of (011) twins; arrows are marked satellites arising for twins in a deflection from the exact Bragg position. *b* — bright-field TEM, 110 projection, acting reflection is $2\bar{2}0$; twin images that are shown have moire pattern, arrow indicate images of precipitate traces. *c* — precipitate and twins caused by stresses arisen at the precipitate/matrix boundary. *a, b* correspond to twins with different {111} planes of location.

(110) in SED investigations and the (010) for HRTEM, FFT and IFFT studies. The (110) projection allows confronting diffraction information concerning APD of different types due to previously uncovered merohedry manifestations. The (010) projection permits excluding the merohedry influence on SED, FFT and IFFT since (101) and $(10\bar{1})$ TB are perpendicular to the projection plane and other TB maybe be eliminated in the HRTEM stage [3,5].

4. SED and TEM studies of $Ca_{0.5}La_{0.5}F_{2.5}$

Specimen preserves a (032) surface plane of the original crystal and has the (110) cleavage plane. Its thickness is ≤ 30 nm that is confirmed by implication with superstructure reflections in peripheral sections SED. Selected orientation and volume correspond to situation in which the reflection state is satisfied for (110) and (101) twins but (011) twins leave the reflection state with the increase of diffraction vectors. Therefore intensity of (011) twin reflections decreases when moving off from the zero series and 5th and 6th reflection series correspond only the (110) and (101) twins. Reflections of the 5th series are suppressed and their positions are marked by asterisks, the 6th series is observed [10].

Specific features of structuring and restructuring of $Ca_{0.5}La_{0.5}F_{2.5}$ are illustrated by Figs. 2–4, 6. All figures correspond to the same crystal, but Fig. 2 conforms to the crystal as a whole, Figs. 3, 4 correspond to FFT and IFFT of some its parts and Fig. 6 contain FFTs and IFFT corresponding to large volumes of the crystal.

Unusual effects are observed in Fig. 2. Firstly, average intensity of StRs of odd reflection series (1st and 3rd) is less than that of even series (2nd and 4th), the 5th series is absent entirely, but StRs of the 6th series are seen distinctly. Secondly, distances between even and odd series (e. g., zero and 1st) along [110] direction are more than between odd and even series (e. g., the 1st and 2nd). Thirdly, $00\bar{2} \rightarrow 1\bar{1}1 \rightarrow 2\bar{2}2$ and $\bar{2}2\bar{2} \rightarrow \bar{1}11 \rightarrow 002$ series are curved symmetrically about $[1\bar{1}1]$ series.

Two anomalies are observed in SED of Fig. 2, *b* and both anomalies are associated with distinctions between characteristics of odd and even series, therefore it can be assumed that both anomalies are provoked by the same reason. Suppression of the odd series and saving of even series can be explained by superposition of one-

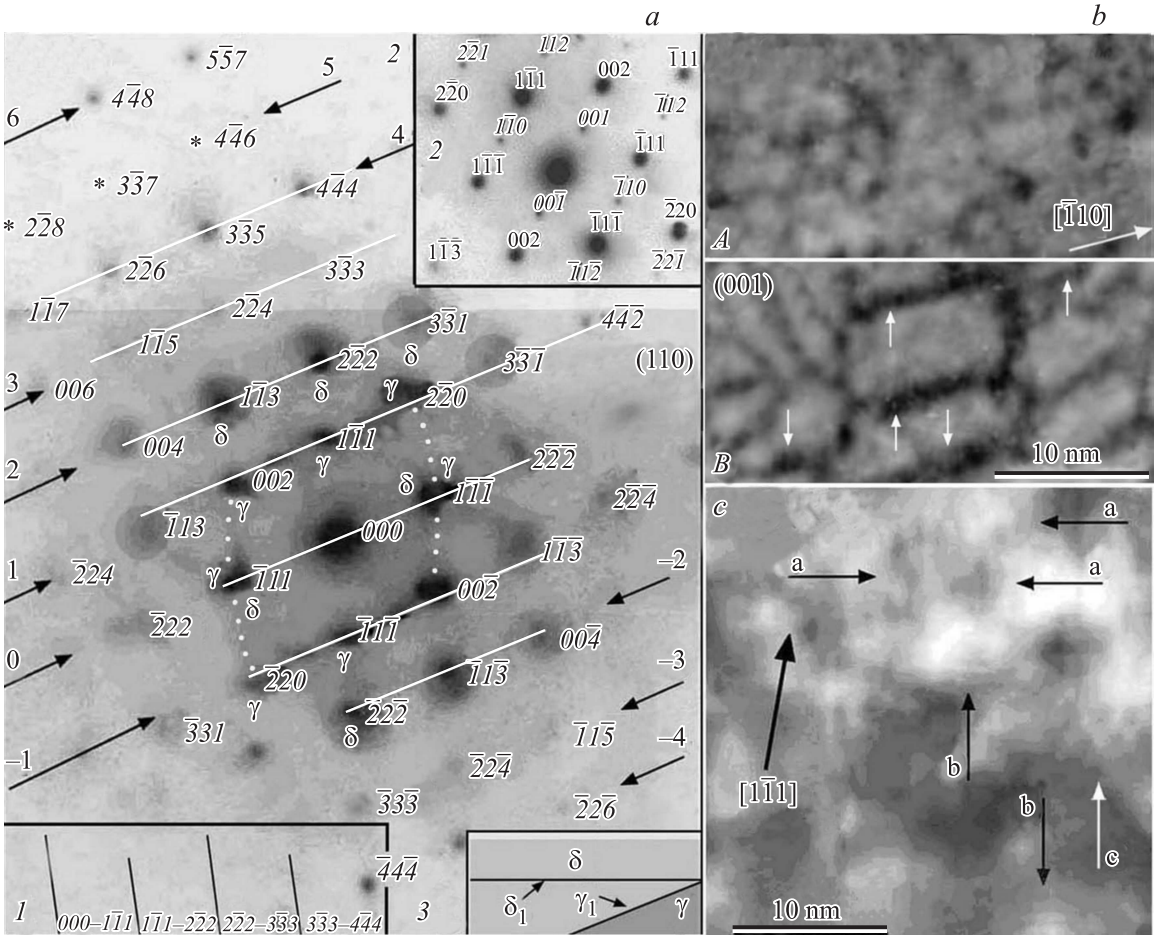

Figure 2. SED and TEMs of $Ca_{0.5}La_{0.5}F_{2.5}$. *a* — SED corresponding to a field with thickness $\sim$ 30 nm and an (110) projection; reflection series are enumerated in order of a distance from the zero series; bright lines go approximately through centers of series; reflections of (110) twins are marked by δ, those of (011) twins are marked by γ: curved reflection series are indicated by spot lines; pairs of single-type reflections (e. g., $\bar{1}13$ and $1\bar{1}3$) belonging simultaneously to odd and even series are marked out by borderings; diffuse halos near 2nd series reflections are sown, Δ — satellites near 1st series reflections; inset *1* — SED of thin area having SStRs; inset *2* — diagram of variations of distances between series along [$1\bar{1}1$] direction; insert *3* — conditional diagram of scattering crystal corresponding to SED. *b*: *A* — bright-field image of cellular structure with hexagonal cells measuring $\sim$ 3 nm, traces of twinning are absent; *B* — bright image of modified structure with increased APD, fringe images of some sectors of ADBs are only possible images of twins; *c* — dark-field image of the cellular structure in $\bar{1}12$ SStR and its satellite, deflection of 0.3° from the true Bragg angle; bright images are APDs; fringes with the 1 nm period corresponding to images of (011) TB (a); those with 0.5 nm period conforming to (110) TB (b); an image with chess contrast corresponds to superposed twins (c).

type reflections belonging to different twins (the merohedry) [6,8].

However {111} twins cannot provoke merohedry, and if the suppression/weakening of the odd series is provoked by twinning, it is necessary to find a corresponding twin. Twinning leads to rotation of a lattice through π about the axis normal to a twinning plate. Vector **a** is transformed in a vector $\mathbf{x}_a$ in the result of the rotation in accordance with equation [6,7,11].

$$\mathbf{x}_a = 2\,\frac{\mathbf{b}(\mathbf{ab})}{b^2} - \mathbf{a}, \qquad (1)$$

were **b** is the rotation axis. In the result, a *hkl* reflection in the FCC lattice or a lattice coming from FCC transforms into $h'k'l'$ reflection, indices of which are defined by equations:

$$h' = 2h\,\frac{hu + kv + lw}{u^2 + v^2 + w^2} - h, \qquad (2a)$$

$$k' = 2k\,\frac{hu + kv + lw}{u^2 + v^2 + w^2} - k, \qquad (2b)$$

$$l' = 2l\,\frac{hu + kv + lw}{u^2 + v^2 + w^2} - l, \qquad (2c)$$

where u, v, w are indices of twinning plane normal.

$1\bar{1}3$, 002, $1\bar{1}1$, $2\bar{2}0$, $3\bar{3}\bar{1}$ reflections are suppressed or weakened in the 1st series. 002 is suppressed if 020 of other twin is superimposed on it, and indexes of equation (1) gain values: $h = 0$, $h' = 0$, $k = 0$, $k' = 2$, $l = 2$, $l' = 0$ at that

equations (2a)–(2c) are transformed in the result of these substitutions in equations:

$$\text{equation(2a)} \to 4uv = 0, \tag{3a}$$

$$\text{equation(2b)} \to (u^2 + v^2 + w^2) = 2vw, \tag{3b}$$

$$\text{equation(2c)} \to w^2 - (u^2 + v^2) = 0. \tag{3c}$$

Totality indexes resulting from equations (3a)–(3c) corresponds to (101) twinning; the $(\bar{1}01)$ twinning also conforms to superposition of $\bar{1}13$ and $\bar{1}31$, etc. Overlap of 002 and 200 results in (011) twinning.

{110} twins are forbidden in FCC structure but the prohibition goes off due to the tetragonality. {110} twinning explains formally the intensity variations in the SED of Fig. 1, but problems of the origin of {110} twins in place of {111} twins and variations of distances between series remain to be resolved. Twinning in solids is inseparably linked with relaxation of stressed state [6,7,11]. Bright- and dark-field TEM indicate that the twinning is inseparably involved with APD, therefore the reason of anomalies can be associated with stresses provided by contacts of DACDs with different tetragonality directions.

Regularities of structuring that arise when different DACDs are conjugated were examined by simulation in the approximation of 2 half-spaces. Tetragonality inherent in DACD is defined as small distortion of the cubic lattice. Tetragonality directions are [001] and [010], conjugation of DACD lattices on (101) interfacing plane is regarded as homogenous. Atom displacement u_i from a cubic lattice with a lattice constant a obeys the equations:
if tetragonality direction is [001]

$$u_x = -\frac{\tau}{4}x - \tau z, \;\; u_y = \frac{\tau}{2}y,$$

$$u_z = \tau z\,\frac{5\lambda_{11} + \lambda_{12} - \lambda_{44}}{4(\lambda_{11} + \lambda_{12} + \lambda_{44})}, \tag{4a}$$

if tetragonality direction is [010]

$$u_x = -\frac{\tau}{4}x, \;\; u_y = \frac{\tau}{2}y, u_z = \tau z\,\frac{\lambda_{11} + 5\lambda_{12} - \lambda_{44}}{4(\lambda_{11} + \lambda_{12} + \lambda_{44})}, \tag{4b}$$

where x, y, z are coordinates, u_x, u_y, u_z — displacements, λ_{11}, λ_{12}, λ_{44} — cubic crystal elastic modulus (as approximate modulus were used the CaF_2 modulus), $\tau = c/a - 1$, c is the constant of a tetragonal lattice. As the result of the solitary twinning boundary, stresses are absent and in accordance with equations (4a), (4b), lattices of conjugated DACDs are distorted mirrorly, a (110) cross-sections serving as a conjugation planes change a configuration from rectangular to parallelogram and APD lattices gain monoclinic distortions.

Angles of monoclinic lattices obtained values in accordance to estimation on the base of equations (4a), (4b) for the tetragonality direction [001]

$$\text{angle } x\widehat{}z \to \arctan\left(\frac{1}{\tau} + \frac{5\lambda_{11} + \lambda_{12} - \lambda_{44}}{4(\lambda_{11} + \lambda_{12} + \lambda_{44})}\right) \approx 87.2^\circ,$$

$$\text{angles } x\widehat{}y = x\widehat{}z = 90^\circ.$$

Complementary angles $z\widehat{}x$ for conjugated APD are equal to $\pm 2.8^\circ$.

Projection (110) contains 2 specific direction: $[\bar{1}1\bar{1}]$ by which the (110) plane is crossed by (101) TBs and $[1\bar{1}\bar{1}]$ by which the (110) plane is crossed by (011) TBs. Satellites near $\bar{1}11$ and $1\bar{1}1$ reflections correspond to (011) twins. Diffuse halo oriented along $[\bar{1}11]$ near 2nd series reflections conform to $(\bar{1}01)$ twins. SED contains all reflection series parallel to $[1\bar{1}1]$ direction, manifestations of the merohedry for these series are excluded, consequently, their reflections are not coinciding, and different tetragonality directions are inherent in (110) and (011) twins. Suppression of odd series is observed along the $[1\bar{1}\bar{1}]$ direction, that is especially obvious for 4th, 5th and 6th series; this suppression is provoked by the superposition of (110) and (101) twin reflections. (110) and (101) twins have identical tetragonality directions and identical diffraction patterns. Only combination of twinning, which is reflected by SED in Fig. 2, *b*, are (110) and (101) twins with common [100] tetragonality direction and (011) twins with the [001] tetragonality direction.

From suggested pattern structuring, it follows that odd series contain solely (011) twin reflections, therefore they carry information concerning a (011) structuring, whereas reflections in even series arise as the result of summing of reflections of all types and, as a first approximation, they can be considered as a source of information concerning (110) structuring. Analysis of SED demonstrates that next equations/inequalities resulting from equations (4a), (4b) are satisfied for its key reflections:

$$\mathbf{g}_{1\bar{1}1\delta} > \mathbf{g}_{\bar{1}11\delta}, \;\; \mathbf{g}_{11\bar{1}\gamma} > \mathbf{g}_{1\bar{1}1\gamma}, \;\; \mathbf{g}_{1\bar{1}1\delta} = \mathbf{g}_{11\bar{1}\gamma}, \;\; \mathbf{g}_{\bar{1}11\delta} = \mathbf{g}_{1\bar{1}1\gamma}. \tag{5}$$

2nd peculiarity of SED related to crossing (110) and (011) twins is bending of a crystal around the direction of twin crossing $[1\bar{1}1]$ that leads to rapid decrease of intensity reflections with distance from $[1\bar{1}1]$. This effect is appreciable in SED but inherent even to a greater extent in FFT.

$Ca_{0.5}La_{0.5}F_{2.5}$ TEMs in Fig. 2, *b, c* have no signs of large-scale twins, but the totality of peculiarities of SED in Fig. 2, *a* proves twinning undoubtedly. Ions F^{+1} in $Ca_{1-x}La_xF_{2+x}$ occupy tetrahedral holes and do not influence the lattice constant. $Ca_{1-x}La_xF_{2+x}$ lattice constant changes linearly from 5.42 up to 5.68 Å when composition changes from LaF_3 to $Ca_{0.6}La_{0.4}F_{2.4}$ [10]. Consequently the relative distinction of ion radii La^{+3} and Ca^{+2} is equal to 10%. Therefore distinctions in tetragonality directions in $Ca_{0.5}La_{0.5}F_{2.5}$ must be accompanied by variations of lattice constants near to 5%. If large-scale twins are realized, stress accumulated in twins must relax with the formation of

misfit dislocations. Absence of dislocations is evidence for nanodimensionality of twinning, and this result is confirmed by the concretion of APDs and twins and by the complete suppression of reflections of the 5th series.

The inequalities of $\mathbf{g}_{1\bar{1}1\delta} > \mathbf{g}_{\bar{1}11\delta}$, $\mathbf{g}_{11\bar{1}\gamma} > \mathbf{g}_{1\bar{1}1\gamma}$ and the equations of $\mathbf{g}_{1\bar{1}1\delta} = \mathbf{g}_{11\bar{1}\gamma}$, $\mathbf{g}_{\bar{1}11\delta} = \mathbf{g}_{1\bar{1}1\gamma}$ have particular meaning. The inequality of single-type diffraction vectors belonging to the same (110) cross-section is not possible in a tetragonal lattice. Therefore the above-listed inequalities prove explicitly that lattice is monoclinic. The above-listed equations prove explicitly that conjugated APD are distorted mirrorly. Resulting structure consists of interdependent interweaving APDs with different directions of monoclinic distortions. Restructuring based on the conjugation of APD with different directions of tetragonal distortions decrease the level of stressed state, at least, partially, but could not lead to equilibrium state since stresses that are provoked by contacts between APD with different directions of monoclinic distortion replace only stresses provoked by contacts between APD with different tetragonality directions.

Subsequent development of structuring must limit stresses provoked by mismatch of lines with different directions of monoclinity. Underlying reason of this transformation follows from the character of conjugation of DACDs with different tetragonality, as result of which structures of the conjugated DACDs undergo mirror distortions. Arising monoclinic distorted DACD lattices have the same deviations from the xy plain normal in magnitude but different in signs. Therefore rotation of any component of arising pair about the axis normal to the xy plain through π calls forth the coincidence of these pairs. This operation in a solid crystal can be realized by twinning.

Twinning can be regarded as the continuous sequence of stacking faults, and a stacking fault is the indispensable nucleus of a twin; although APB is interpreted as stacking faults [3] they cannot have a twin nucleus. Therefore twinning in $Ca_{1-x}La_xF_{2+x}$ is associated with the prior stacking fault generation. The origin of a stacking fault is the critical moment of the whole process of twinning since a process of the stacking fault origin demands in the ordinary conditions stresses $\sigma = 0.1\mu$. Three factors facilitate this generation in $Ca_{0.5}La_{0.5}F_{2.5}$: firstly, $Ca_{1-x}La_xF_{2+x}$ solid solutions have small stacking fall energy as stated above; secondly, misfit stresses at boundaries APDs with different directions of monoclinic distortions can relax by means of twinning; thirdly, a high level of the cumulative energy associated with APB that also was noted before demands relaxation.

Twin initiation is illustrated in this paper by an example of the realization of the shuffled dislocation mechanism, although similar results could also be obtained in other twinning mechanisms. Glide and climb of shuffled dislocations extend the displacement inherent in a stacking fault on modifiable volume integrally, transforming it into a twin relative to an unmodified volume. (110) twinning is proved irrefutably by the SED regularities, twinning traces are observed at APB, but any traces twins or residual APB inside increased APD are absent. Reciprocal annihilation of APD and twins is only possible explanation of this phenomenon. However it must satisfy additional conditions: firstly, a twinning plane must coincide with the APB plane; secondly, a shuffled dislocation must nullify the displacement at APD.

If a twin must eliminate the (110) APB owning to $(1/2)[1\bar{1}0]$ displacement, it must theoretically have incoherent type and have the shuffled dislocation with $(1/2)[1\bar{1}0]$ the Burger's vector. Similar twin implements a triple operation: firstly, APB is eliminated, secondly, it is recovered correct alternation of components in going from the unmodified volume to the twin, thirdly, a current monoclinic line is refracted and a lattice of refracted volume appears parallel to a lattice of another member of initial monoclinic pair.

Described regularities of restructuring are proved exhaustively by FFT and IFFT.

5. HRTEM, FFT and IFFT studies of $Ca_{0.5}La_{0.5}F_{2.5}$

Results of $Ca_{0.5}La_{0.5}F_{2.5}$ investigations by HRTEM, FFT, IFFT are given in Figs. 3–5 and 6. Figs. 3 and 4 belong to two areas of the same crystal. However Fig. 3 corresponds to area where a few domains with different tetragonality directions collide and a faulty field arises. Stresses state of this field blocks subsequent structuring and APD structure freeze. Fig. 4 corresponds to area remote from the faulty fields, therefore reconstruction processes have no limitation in it. Fig. 5 contains diagrams, illuminating transition from the structure with 2 monocline lines to the structure with an unitary corrugated line. Fig. 6 corresponds two vast volumes: APD structure prevails in the Fig. 6, *a*, restructuring dominates in the Fig. 6, *b* and *c*.

6. Influence of faulty structure on $Ca_{0.5}La_{0.5}F_{2.5}$ structuring

HRTEM of APD structure are shown in Fig. 3, *a*; the image corresponds to reflections shaded in insert; A, B, C are conjectural APDs; conjectural domain boundaries are shaded; *1* and *2* are conjectural APBs, their basic tokens have diffuse tails along with pitted points; *3* is conjectural boundary between DACDs, its basic tokens are superfluous, forked, wrong points; *4* is faulty area arising as a result of contacts of a few DACDs and APDs, its basic tokens are identical with the tokens of the 3rd boundary. In Fig. 3, *b* FFT corresponding to HRTEM in Fig. 3, *b* is shown; presence of superstructure reflections is an evidence of ordering; pattern of satellites and spikes in the neighbourhood of the 000 lattice site reflects APD structure; the axis of the satellite pattern is aligned with the $2\bar{1}0-\bar{2}10$ line (the direction between similar ions in neighbouring APD) and rotated through 20.7° about axis of the reflection pattern; $\mathbf{g}_s = (1/4)\mathbf{g}_r$

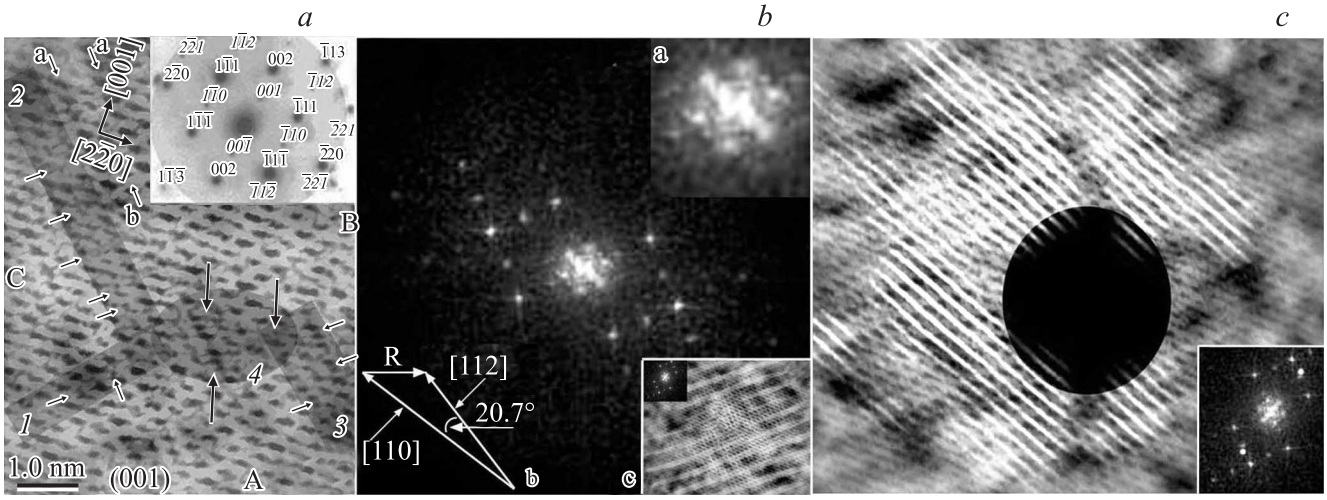

Figure 3. Influence of faulty structure on $Ca_{0.5}La_{0.5}F_{2.5}$ structuring.

($\mathbf{g}_s$ is satellite diffraction vector, $\mathbf{g}_r$ is $\mathbf{g}_{2\bar{1}\bar{0}}$) that reflects a projection of the $[2\bar{2}0]$ on the $2\bar{1}0-\bar{2}10$ line. Inset a shows extended image of the central area. Inset b presents a diagram explaining the 20.7° turn and the $\mathbf{g}_s$ modulus. Insert c shows IFFT conforming to $1\bar{2}0-\bar{1}20$ reflections, having an image of the faulty area; the faulty area breaks fringes, but their linearity remains invariable. In Fig. 3, *c* IFFT with APD images are shown, APD drawn along the direction of shift in the AB plane; longitudinal size is equal to ~ 18 nm, transversal 10 nm. The highest intensity of the satellite pattern reflects the highest level of development of the APD structure (a scale is equal to ≥ 3 nm).

7. Peculiarities of $Ca_{0.5}La_{0.5}F_{2.5}$ structuring in faultless environment

Results of studies of structure corresponding to a field remote from the faulty area are shown in Fig. 4.

8. Joint analysis of Figs. 3 and 4

Preliminary conclusions: 1) all structural peculiarities are realized in the same crystal; 2) the faulty structure promotes preservation of APD structure; 3) moving away from faulty structure one observes restructuring. Detailed mechanism of this is yet in prospect, but it gives large advantages even in having property: firstly, it allows to exclude assumptions that distinctions of observed phenomena are associated with distinctions in compositions; secondly, that distinctions of observed phenomena are associated with distinctions in structural states.

All peculiarities of Fig. 3 are evidence of APD structure of this volume. They coincide even in details: the same APD planes, the same displacement vectors, similar sizes of APD, and so on. The most important information contains in FFT (data is given in respect to the reciprocal space): a displacement vector is [220] (ϖ), the scale of satellite pattern is $(1/4)\,\mathbf{g}_{2\bar{1}\bar{0}}$, most intensive satellites are satellites near to [220] (found on the base of position ω), a satellite pattern is rotated through 20.7° about axis of the reflection pattern.

It seems surprising that structuring of areas remote from the faulty fields differs from structuring of the latter. HRTEM in Fig. 3, *a* and IFFT in Fig. 3, *c* correspond to APD structure, whereas HRTEM in Fig. 4, *a* and IFFT in Fig. 4, *c* conform to uniform structure (at worst to structure with large-scale APDs). FFT corresponding to the area is depicted in Fig. 4, *a*; reflection pattern is distorted and transformed into a parallelogram, whereas the pattern in Fig. 3, *a* corresponds to a cubic lattice. Direction to the 200 reflection in Fig. 4, *b* forms the angle equal to 5.6° with the 200 diffraction vector in a cubic lattice (that conforms to the doubled supplementary angle of the monoclinic lattice). Scale of the satellite pattern in Fig. 4, *b* is halved in comparison with the scale of the satellite pattern in Fig. 3, *b*; therefore a scale of patterns of cells of indeterminate nature in the straight space is at a twofold rate of the APD scale. Satellite pattern intensity in Fig. 4, *b* is weakened, that is an evidence of its small density, but its orientation about diffraction pattern remains invariable. Spikes in the 000 lattice site vicinity observed in Fig. 3, *b* vanish, but there are observed weak spikes between reflections; these spikes are connected to many reflections. Change of spike orientation means a change of boundary orientation. Some superstructure reflections (γ, γ_1, δ, ε) are split and their increased images are observed in corresponding insets. Each superstructure reflection of these pair is bounded with own structure reflection, and this bond becomes apparent distinctly owing to new spikes, each spike is also forked, and each structural reflection connects

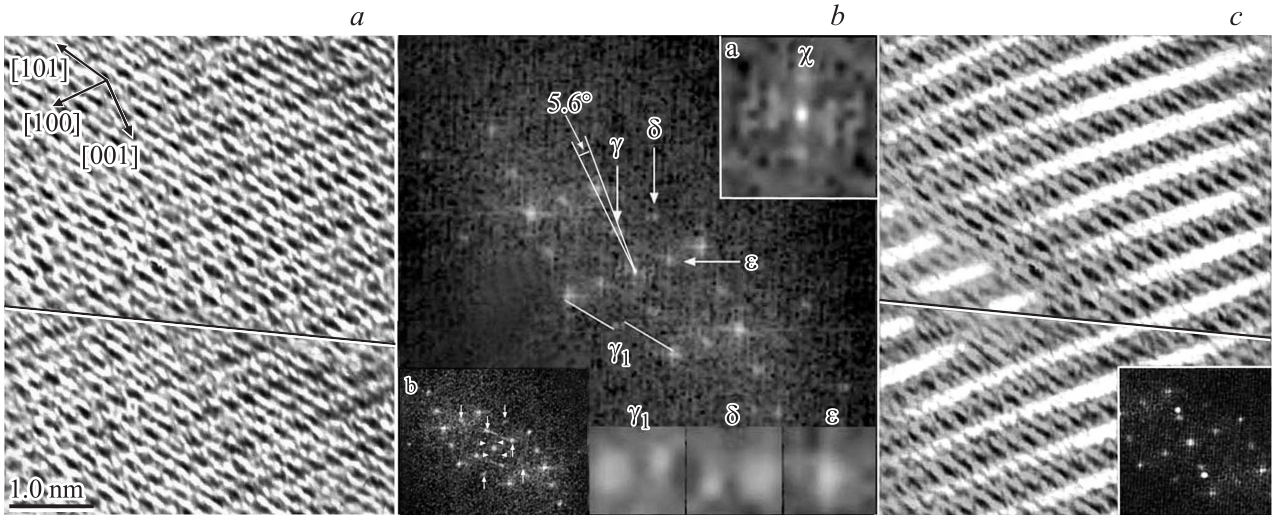

Figure 4. *a* — HRTEM of a field remote from the faulty area; tokens of APD structure are absent; there is discernible superposition of 2 twins, that is explicitly marked by a bright white line; tokens of ordering are slightly depressed in comparison with Fig. 3, *a*. *b* — description of FFT is expounded to avoid tautology simultaneously with evidences of difference between peculiarities of structuring characterized by Figs. 3, *a* and 4, *a*. *c* — IFFT conforming to *a* and *b*; it is observed a partially restructuring area with a large APD arising due to coalescence of initial APDs and a small residual APD; longitudinal size is equal to ~ 18 nm, transversal 10 nm; the highest intensity of the satellite pattern reflects the highest level of development of the APD structure (a scale is equal to ≥ 3 nm).

with own superstructure reflection by means of own portion of a forked spike.

9. Peculiarities of structuring of $Ca_{0.5}La_{0.5}F_{2.5}$ following from results of its studies and possible character of the process

Growth of APD in a process of annealing is an usual process. It is performed by means of absorption of one APD by another due to the movement of APB. Process continues theoretically as long as the cumulative APB energy is not equalized with energy that is necessary for the movement of an APB. However residual APD structure must remain still and any manifestation of HRTEM, FFT, IFFT similar to observed in Fig. 3 must remain still as well. Nevertheless the hypothesis concerning traditional APD relaxation cannot explain multiple peculiarities of Fig. 4, *b*: diffraction pattern in the parallelogram shape; the deflection of $\mathbf{g}_{2\bar{1}0}$ equal to 5.6° from the normal position; anomalous sizes of a satellite pattern and standard its orientation; selective splitting of some reflections and spikes, presence of bonds between structural and superstructural reflections.

Therefore it is necessary to study the possibility of explanations of listed anomalies on the base of the hypothesis about the APB annihilation in the result of twinning of the merohedral type. At that, it is necessary to pay attention to the fact, that the initial cause of twinning is associated with the relaxation of stresses provoked by APD with monoclinic distortion. Theoretical diagram explaining possible effect is given in Fig. 5.

Change of structuring leads to change of diffraction pattern. Firstly, most evident effect is departure of the ϖ position from the ω position, the departure corresponds to theoretically calculated value 5.6° (that exceeds multitude mistakes in positions of reflections observed in other diffraction patterns). Secondly, it is inexplicably splitting of reflections, that is especially visibly for weak superstructure

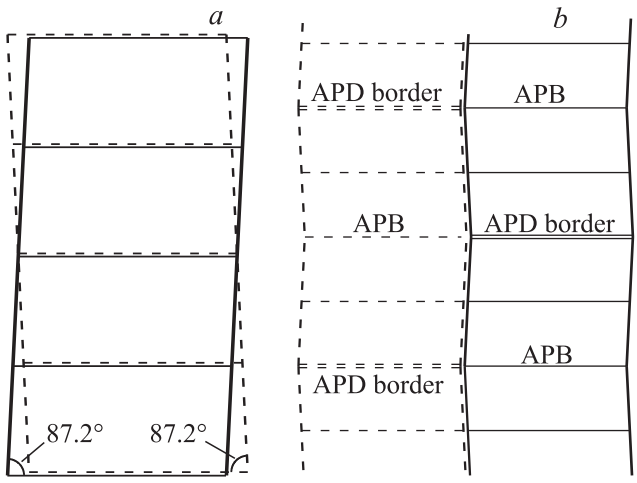

Figure 5. *a* — diagram of conclusive stage of obtaining energetic advantageous structuring of ordered solid solution on the base of component with different atomic radii. *b* — diagram in which, there are conventionally superimposed lattices with different directions of monoclinity. Alternation twins allow elimination of misfit stresses. APB borders are APB planes where the turning point lattice is realized.

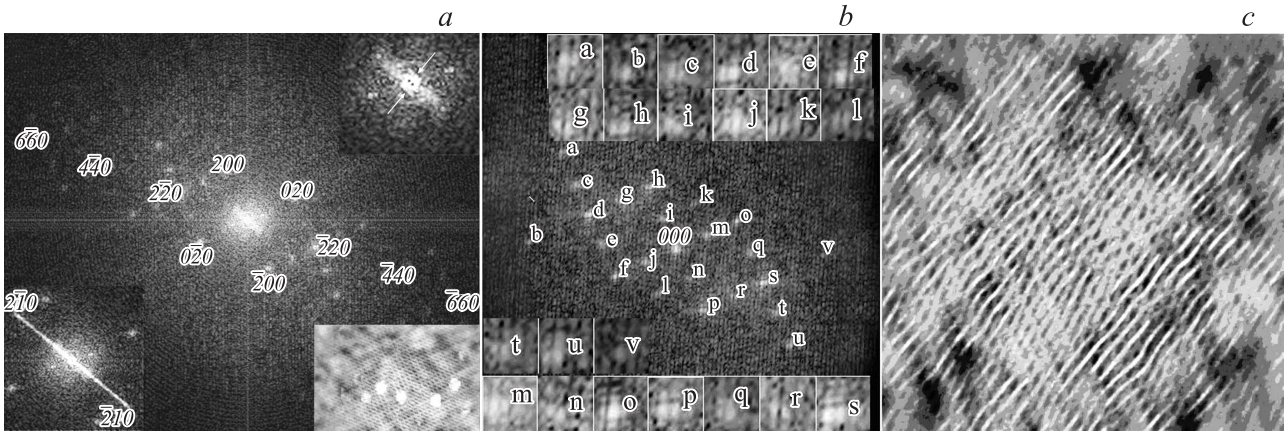

Figure 6. FFT and IFFT of large parts of the crystal. *a* — corresponds thick field with large density of faulty areas (explicitly marked by bright white points in the inset of Fig. 3, *b*; FFT retains appearance typical for Fig. 3, *b*. *b* — FFT corresponding the thin area; satellite picture is absent completely; structural and superstructure reflections are forked; it corresponds to superposition of reflections of 2nd half of a pattern (the forked is seen clear in insets). *c* — IFFT corresponds to *b*; against a background, where curves of fringes are provoked by curves and variations of thickness of crystal, there are clear breaks and 6° arches corresponding to actions of twinning.

reflections, at that a direction of splitting reflects to the orientation change. Thirdly, not only the reflections split but also spikes, at that, splitting spikes forms bridges that unite structural an superstructural reflections that belong to the same half of FFT. All indicated (and the some unnamed) peculiarities prove that APB annihilation was stimulated by the (110) twinning.

Diffraction lattices separated by former boundary acquire regularities. Most evident of which is effect of divergence of the ϖ position from the ω position, at that the displacement corresponds to theoretically calculated value 5.6° (it exceeds multitude mistakes in positions of reflections observed in other diffraction patterns). It is also necessary to explain a peculiar splitting of reflections, that is especially visible for weak superstructure reflections and a direction of splitting reflects the orientation change. It is also necessary understand the effect of splitting of not only reflections but also spikes, at that, spikes splitting forms bridges that unite structural an superstructural reflections that belong to the same half of FFT.

However there are other effects going beyond the scope of discussed model and given important data. Double decreasing of the satellite pattern itself without further intricate constructions means that an unusual process is observed. This effect is associated with a mechanism of structuring but according to preliminary data it has no a relationship to the main problem of the investigations concerning minimization of cumulative energy.

10. Place of two types of structuring in the scale of the crystal as a whole

Information obtained by SED and TEM is concerned, at least, to large parts of the crystal. Results obtained by HRTEM, FFT and IFFT techniques concerned small areas and consequently it is necessary to determine: the role of found peculiarity of structuring in the scale of the whole of the crystal. Two large parts of the crystal were studied by HRTEM, FFT and IFTT. The 1st of these fields corresponds approximately to the area used for obtaining SED. More thin part of the crystal, located near its edge was selected for the 2nd field. FFT represented in Fig. 4, *b* was obtained approximately from an area located in the centre of the 2nd field.

Saddle-shaped bend of the crystal is a clear evidence in studies of spacious volumes, where the bend affects a shape of pattern. EPDs contain only selection diffractions. Only reflections belonging to the (110) projections predominate on Fig. 6, that is especially important for Fig. 6, *b* and *c*. Reflections of spitting pairs in Fig. 6, *b* are displaced along the $[2\bar{1}0]-[\bar{2}10]$ direction and belong to the pairs that arise as a result of APD with [010] and [001], therefore observed displacements correspond to symmetric turns rising in the adjunctions and prove the present of existence of quasi-merohedry. Results of investigations are depicted in Fig. 6.

All peculiarities in Fig. 6, *a* correspond to the average over a volume where a prevailing component of structure is APD. Fig. 6, *b* has no manifestations of APD. Not taking into account a comparison between Fig. 6, *a* and *b*, Fig. 6, *b* looks like an usual pattern of ordering massif. Reflection bifurcation with a constant distance between reflections (there are even triple reflections, where 2 satellites are placed symmetrically relative to the centre) cannot arise from APD structure in a usual way. Theoretically similar structure can be created artificially, but structuring in Fig. 6, *b* arises as the result of self-organization. Disclosure of splitting of all reflections is the strong evidence, that crystal is mosaic of APD, with different monoclinity directions, and netting

of fringes with $\sim 6^\circ$ windings which are absent in other IFFT and which are not manifestations in FFT Fig. 6, *b* is a definite proof of the mosaic structure of the crystal. Unusual image of this structure is observed in Fig. 6, *c*. Similar structure is not known in literature.

11. Conclusion

General result of investigations is the proof of adequacy of process of elimination of cumulative energy as the result of series of successive acts: ordering, APD formation, relaxation of misfit energy by means of formation mirror monoclinic structures, repeated relaxation of elastic energy associated with monoclinic structures be means of twinning of the quasi-merohedral type.

Investigations were carried out on $Ca_{1-x}La_xF_{2+x}$ that is an ordered solid solution where APB arises due to the stochastic character of ordering of solid solutions. Compounds arise as a result of equilibrium processes and a rigid sequence of component alternations is attributed to them. However a non-regular component alternation can arise as a result of non-equilibrium processes, provoking the origin of volumes separating boundaries similar to APB. Origin of APD in compounds is associated with the kinetics but not with the thermodynamics, i. e., it is the problem of technology. These APD are not important for the explanation of the physical and chemical properties of a substance, although they are important for creation of reproducible technologies. Both the quasi-merohedry and the phase summing must affect results of the refinement. Probably, we are mistaken but we have no found studies devoted to an origin or lack of origin of APB in processes of compound syntheses. Possibly, similar generalizing studies are impossible by virtue of the infinite number of synthesis conditions and every synthesis process must be studied personally, that is especially important in nanotechnologies, which are non-equilibrium in the most cases.

Phenomenon is found in $Ca_{0.5}La_{0.5}F_{2.5}$ solid solution where its revealing has been favoured by join characteristics unknown in other compositions: APD measuring in 3 nm and a record distinctions of ion component radii equal to 10%. However ordering solid solutions are usual spices and this effect must arise undoubtedly in many other compositions, imparting new properties of compositions and confusing results of structure researchers. Micrographs conforming vast volume correspond satisfactory to images of small areas and results as a whole.

Authors have not met structures where (110) twins serve twofold function: joining layers with different symmetry and uniting layers that were divided before by APB. It can be a new structural state. Possibility of existing of different phases in the same crystal allows to make new devices or to improve the existing. Multiphasic states expand device capabilities.

References

[1] A. Cooksy. *Physical Chemistry: Thermodynamics, Statistical Mechanics, and Kinetics* (Prentice Hall, Boston, 2013).
[2] A. Barnard. Rep. Progr. Phys., **73** (8), 86 502 (2010).
[3] J. Friedel. *Dislocations* (Pergamon Press, Oxford, 1967).
[4] S.K. Maksimov, K.S. Maksimov. Inorg. Mater., **43**, 551 (2007).
[5] S.K. Maksimov, K.S. Maksimov. Bull. Rus. Acad. Sci. Phys., **75**, 1176 (2011).
[6] J. Hirth, J. Lothe. *Theory of dislocations* (McGraw-Hill, N.Y., 1968).
[7] A.G. Khachaturyan. *Theory of structural transformations in solids* (Dover Publications, N.Y., 2008).
[8] B. Maximov, H. Schultz. Acta Crystallogr., **D41**, 88 (1985).
[9] B.P. Sobolev. *The rare earth trifluorides* (Institut d'Estudis Catalans, Barcelona, 2000).
[10] S.K. Maksimov, K.S. Maksimov. J. Surf. Invest.: *X*-ray, Synchrotron Neutron Tech., **9** (2015) (in Press).
[11] N.I. Vlasova, G.S. Kandaurova, L.G. Onoprienko, N.N. Shchegoleva. Sov. Phys. Usp., **35**, 420 (1992).

Редактор Л.В. Шаронова